
Article:
Moscholios, Ioannis, Vasilakis, Vasileios orcid.org/0000-0003-4902-8226, Sarigiannidis, Panagiotis et al. (2 more authors) (2018) An analytical framework in LEO mobile satellite systems servicing batched Poisson traffic. Iet communications. pp. 18-25. ISSN 1751-8628

https://doi.org/10.1049/iet-com.2017.0220

An Analytical Framework in LEO Mobile Satellite Systems Servicing Batched Poisson Traffic

I. D. Moscholios[1,*], V. G. Vassilakis[2], P. G. Sarigiannidis[3], N. C. Sagias[1], M. D. Logothetis[4]

[1]Dept. of Informatics & Telecommunications, University of Peloponnese, 221 31 Tripolis, Greece.
[2]Dept. of Computer Science, University of York, YO10 5GH York, U.K.
[3]Dept. of Informatics & Telecommunications Engineering, University of Western Macedonia, 501 00 Kozani, Greece.
[4]WCL, Dept. of Electrical & Computer Engineering, University of Patras, 265 04 Patras, Greece.
[*]idm@uop.gr

Abstract: We consider a low earth orbit (LEO) mobile satellite system (MSS) that accepts new and handover calls of multirate service-classes. New calls arrive in the system as batches, following the batched Poisson process. A batch has a generally distributed number of calls. Each call is treated separately from the others and its acceptance is decided according to the availability of the requested number of channels. Handover calls follow also a batched Poisson process. All calls compete for the available channels under the complete sharing policy. By considering the LEO-MSS as a multirate loss system with "satellite-fixed" cells, it can be analyzed via a multidimensional Markov chain, which yields to a product form solution (PFS) for the steady state distribution. Based on the PFS, we propose a recursive and yet efficient formula for the determination of the channel occupancy distribution, and consequently, for the calculation of various performance measures including call blocking and handover failure probabilities. The latter are much higher compared to the corresponding probabilities in the case of the classical (and less bursty) Poisson process. Simulation results verify the accuracy of the proposed formulas. Furthermore, we discuss the applicability of the proposed model in software-defined LEO-MSS.

1. Introduction

Satellite systems have been deployed as an attractive solution to provide high-quality broadband communication services to both fixed and mobile terminals. Based on the Earth's surface proximity, low earth orbit (LEO) mobile satellite systems (MSS) have nowadays regained increased interest especially by the satellite industry. In this context, Iridium is currently developing, and has already launched the first ten of at least seventy satellites of Iridium NEXT, a second-generation worldwide network of LEO satellites. Other private companies, such as SpaceX and OneWeb, are currently planning to launch more than 4000 and 650 of LEO satellites, respectively, forming mega-constellations, in order to provide global high-speed internet connectivity. These ventures are the biggest challenges in the satellite communications business today. In this direction, European Space Agency has recently also announced its dedicated support to the development of such large LEO constellations. In contrast to geostationary earth orbit (GEO) satellites, the low altitude of LEO-MSS makes them ideal for providing multiservice real-time applications to a diverse population, while their multitude ensures global coverage [1]. Comparing LEO to GEO satellites, the

former ones are less expensive, require less transmission power, while suffering from lower free space losses and shorter transmission delays. The expense, however, is higher network complexity and frequent beam handovers (that occur due to the high speed of LEO satellites) to in-service fixed or mobile users (MUs).

An important aspect of contemporary LEO-MSS is their ability to accommodate calls of different service-classes. For a precise analysis of the call-level performance of LEO-MSS, the selection of the appropriate teletraffic model is, thus, essential for a number of reasons. First, the utilization of an appropriate teletraffic model will be helpful in order to track subtle differences of call-level traffic characteristics and also to assure high quality-of-service (QoS) among different service-classes. More importantly, with such a model, reliable analytical results for various performance measures under consideration can be extracted, including handover failure and call blocking probabilities (CBPs). As a further advantage, a special category of teletraffic models is the ones having the ability to yield in recursive formulas that are efficient in terms of computational complexity. Thus, such models can be invoked in satellite network planning and dimensioning procedures. In addition, two emerging and complementary to each other technologies are software-defined networking (SDN) and network function virtualization (NFV). SDN decouples the control plane from the data plane and centralizes control and programmability of the network. NFV transfers network functions from dedicated appliances to generic physical infrastructure. Since both have the capacity to significantly enhance network performance, and thus, reduce overall costs, they are considered as new standards in design, operation and management of next-generation communication satellite networks [2, 3]. Hence, following these recent advances of network technologies, future teletraffic models should also attain another advantage of being applicable in the architectural and functional enhancements of SDN/NFV enabled satellite networks.

In the open technical literature, various teletraffic loss or queueing models have been introduced for the call-level analysis of LEO-MSS (e.g., [4]-[15]). These models can be classified based on various critical intrinsic characteristics, such as the channel sharing policy, the existence of queues or not, etc. In the next two paragraphs, the most relevant teletraffic models to LEO-MSS are cited, shortly discussed and classified as single-rate (e.g., [4]-[12]) and multirate (e.g., [13]-[15]). This classification has been made not only for simplicity of their presentation but also in order to show that few models exist in the case of multirate satellite traffic.

Starting with the single-rate models, in [4], each cell is modelled as a Markovian loss-queueing model that accommodates Poisson arriving calls (new or handover), which require a single channel in order to be accepted in the cell. To guarantee a certain QoS to handover calls, a fixed channel reservation (FCR) policy is considered, named as channel-locking mechanism, which treats differently the first call handover from the subsequent ones. Extensions of [4] are numerous and related to schemes based on: i) dynamic channel reservation with [5] or without [6] priorities, ii) time-based channel reservation [7, 8] iii) Doppler-based handover prioritization [9, 10], iv) probabilistic reservation for the handover management [11] and v) FCR with first-in-first-out queueing handover [12].

Regarding the multirate models, in [13], an analytical framework has been proposed for evaluating the performance of the complete sharing (CS) and the FCR policies that are applied in LEO-MSS, with "satellite-fixed" cells, supporting multirate Poisson traffic. Under the CS policy, all calls have access to the available channels. A call is accepted in a cell whenever the required channels are available. Otherwise the call is blocked and lost. In [14], apart from the CS and the FCR policies, the complete partitioning (CP) and the threshold call admission (TCA) policies have been further proposed. In the CP policy, the capacity C (in channels) of a cell is partitioned into K

subsets, where K is the number of service-classes accommodated in the cell and C_k is the capacity of each partition. In each class k ($k = 1, \ldots, K$), a certain partition is allocated. Thus, each cell can be modelled as an $M/M/C_k/C_k$ system. In the TCA policy, new service-class k calls are not allowed to enter a cell, if the number of in-service new and handover calls of service-class k plus the new call exceeds a threshold (different for each service-class). In [14], simulation results have been presented for the TCA policy. In [15], an analytical Markovian model has been proposed for the TCA policy that allows the determination of CBP and handover failure probabilities.

A common assumption in all the aforementioned papers is that the call arrival process of both new and handover calls follows the original Poisson process. Although this assumption usually results in analytically tractable formulas, it is only a coarse approximation, since it can not capture the bursty nature of traffic, emerged in LEO-MSS [16]-[18], as the batch Poisson process can do. This versatile process is quite important not only because calls may arrive as batches in many LEO-MSS applications, but also because it can be used in cases where arrival processes are more peaked and bursty than the Poisson process [19].

Motivated by the above observation, in this paper, we consider the bursty nature of multirate traffic created in LEO-MSS at call-level. Specifically, the batched Poisson process is adopted, which, to the best of our knowledge, has not been used in LEO-MSS yet to accurately model multirate bursty traffic. More precisely, we model a LEO-MSS as a multirate loss system that accommodates calls of different service-classes. New calls of a service-class arrive in the system according to a batched Poisson process with generally distributed batch size. Calls of a new batch are treated separately from the rest ones, which means that one or more calls of a batch can be accepted in the system, while the rest can be blocked and lost, due to lack of available channels (CS policy). Considering handover calls, we also assume that they follow a batched Poisson process. Our contributions are summarized as follows:

- We first show that the model under consideration can be analyzed via a multi-dimensional Markov chain and then provide a product form solution (PFS) for the calculation of the steady state probability distribution.
- A recursive formula for the calculation of the channel occupancy distribution is derived, that facilitates the extraction of performance measures such as CBP and handover failure probabilities.
- We introduce a framework for the applicability of the proposed model in LEO SDN/NFV satellite networks. Although the presented analysis is not limited to a specific LEO-MSS, we henceforth adopt the Iridium LEO-MSS [20].

The remainder of this paper is as follows: In Section 2, we introduce the LEO-MSS model and provide the various system parameters used in the paper. In Section 3, we present the proposed model and prove: i) the PFS of the steady state distribution (Section 3.1) and ii) a recursive formula for the calculation of the channel occupancy distribution (Section 3.2), based on which all performance measures are determined. In Section 4, we discuss the applicability of the proposed model in SDN/NFV enabled LEO satellite networks. In Section 5, we present analytical and simulation results of the proposed model and compare them, for evaluation, with the analytical results obtained in [13, 14] for various performance measures. The comparison of the analytical results obtained by the proposed model with the corresponding simulation results shows an absolutely satisfactory accuracy. In Section 6, we present the conclusions. To facilitate the paper's readability, we include a list of all abbreviations in Appendix 1.

2. The LEO-MSS model

We consider a LEO-MSS of N contiguous "satellite-fixed" cells, each having a fixed capacity of C channels. Moreover, each cell is modelled as a rectangle of length L (425 km in the case of the Iridium LEO-MSS [20]), that forms a strip of contiguous coverage on the region of the Earth. Next, a few common assumptions are made: LEO satellite orbits are polar and circular. MUs are uniformly distributed on the Earth surface, while they are considered as fixed. This assumption is valid as long as the rotation of the Earth and the speed of a MU are negligible compared to the subsatellite point speed on the Earth [4]. Moreover, either beam handovers, within a particular footprint, or handovers between adjacent satellites of the same orbit plane may occur. Note that all the above assumptions are valid for the Iridium LEO-MSS.

The system of these N cells accommodates MUs who generate calls of K service-classes with different QoS requirements. Each service-class k $(k = 1, \ldots, K)$ call requires a fixed number of b_k channels for its whole duration in the system. New service-class k calls arrive in the system according to a batched Poisson process with arrival rate λ_k and batch size distribution $B_m^{(k)}$, where $B_m^{(k)}$ is the probability that a new batch consists of m calls. If $B_m^{(k)} = 1$ for $m = 1$ and $B_m^{(k)} = 0$ for $m > 1$, then a Poisson process results. Due to the uniform MUs distribution, new calls may arrive in any cell with equal probability. The cell that a new call originates is the source cell. Due to the call arrival process of new service-class k calls, we model the arrival process of handover calls of service-class k via a batched Poisson process with arrival rate λ_{hk} and batch size distribution $B_m^{(hk)}$, where $B_m^{(hk)}$ is the probability that a handover batch consists of m calls. The arrival of handover calls in a cell is as follows: handover calls cross the source cell's boundaries to the adjacent right cell having a constant velocity of $-V_{tr}$, where V_{tr} (approx. 26600 km/h in the Iridium constellation) is the subsatellite point speed. An in-service call that departs from the last cell (cell N) will request a handover in cell 1, thus having a continuous cellular network (Fig. 1).

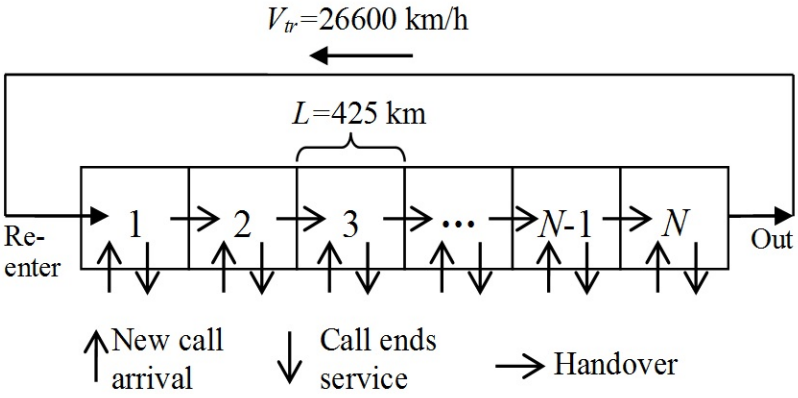

Fig. 1: A rectangular cell model for the LEO-MSS network

Based on the above, let t_c be the dwell time of a call in a cell (i.e., the time that a call remains in the cell). Then, t_c is: (i) uniformly distributed between $[0, L/V_{tr}]$ for new calls in their source cell and (ii) deterministically equal to $T_c = L/V_{tr}$ for handover calls that traverse any adjacent cell from border to border. Based on (ii), T_c expresses the interarrival time for all handovers subsequent to the first one. As far as the duration of a service-class k call (new or handover) in the system and the channel holding time in a cell are concerned, we assume that they are exponentially distributed with mean T_{dk} and μ_k^{-1}, respectively.

To determine formulas for the handover arrival rate λ_{hk} and the channel holding time with mean μ_k^{-1} of service-class k calls, we define:

1. The parameter γ_k, as the ratio between the mean duration of a service-class k call in the system and the dwell time of a call in a cell [4]

$$\gamma_k = T_{dk}/T_c \tag{1}$$

2. The time $T_{h1,k}$, as the interval from the arrival of a new service-class k call in the source cell to the instant of the first handover. $T_{h1,k}$ is uniformly distributed between $[0, T_c]$ with probability density function (pdf) [21]

$$f_{T_{h1,k}}(t) = \begin{cases} \dfrac{V_{tr}}{L}, \text{ for } 0 \leq t \leq \dfrac{1}{\gamma_k} T_{dk} \\ 0, \text{otherwise} \end{cases} \tag{2}$$

3. The probabilities $P_{h1,k}$ and $P_{h2,k}$ that express the handover probability for a service-class k call in the source cell and in a transit cell, respectively. These probabilities are different due to the different distances covered by a MU in the source cell and in the transit cells. More precisely, $P_{h1,k}$ is defined as

$$\begin{aligned} P_{h1,k} &= \int_0^\infty \Pr\{t_{dk} > t | T_{h1,k} = t\} f_{T_{h1,k}}(t) dt \\ &= \int_0^\infty e^{-t/T_{dk}} f_{T_{h1,k}}(t) dt = \gamma_k (1 - e^{-(1/\gamma_k)}) \end{aligned} \tag{3}$$

where t_{dk} is the service-class k call duration time (exponentially distributed with mean T_{dk}). The residual service time of a service-class k call after a successful handover request has the same pdf as t_{dk} (due to the memoryless property of the exponential distribution [22]). It follows then that $P_{h2,k}$ can be expressed by

$$P_{h2,k} = \Pr\left\{t_{dk} > \frac{L}{V_{tr}}\right\} = 1 - \Pr\left\{t_{dk} \leq \frac{L}{V_{tr}}\right\} = 1 - \int_0^{T_c} \frac{1}{T_{dk}} e^{-t/T_{dk}} dt = e^{-(1/\gamma_k)} \tag{4}$$

The handover arrival rate λ_{hk} can be related to λ_k by assuming that in each cell there exists a flow equilibrium between MUs entering and MUs leaving the cell. In that case, we may write the following flow equilibrium equation (MUs entering the cell = MUs leaving the cell)

$$\lambda_k(1 - C_{b_k}) + \lambda_{hk}(1 - P_{f_k}) = \lambda_{hk} + \lambda_k(1 - C_{b_k})(1 - P_{h1,k}) + \lambda_{hk}(1 - P_{f_k})(1 - P_{h2,k}) \tag{5}$$

where: C_{b_k} refers to the CBP of new service-class k calls in the source cell and P_{f_k} refers to the handover failure probability of service-class k calls in transit cells. The values of C_{b_k} and P_{f_k} will be determined in Section 3.

The left hand side of (5) refers to new and handover service-class k calls that are accepted in the cell with probability $(1 - C_{b_k})$ and $(1 - P_{f_k})$, respectively. The right hand side of (5) refers to: 1) service-class k calls that are handed over to the transit cell (depicted by λ_{hk}), 2) new calls that complete their service in the source cell without requesting a handover (depicted by

$\lambda_k(1-C_{b_k})(1-P_{h1,k})$) and 3) handover calls that do not handover to the transit cell (depicted by $\lambda_{hk}(1-P_{f_k})(1-P_{h2,k})$).

Equation (5), can be rewritten as

$$\frac{\lambda_{hk}}{\lambda_k} = \frac{(1-C_{b_k})P_{h1,k}}{1-(1-P_{f_k})P_{h2,k}} \tag{6}$$

To derive a formula for the channel holding time of service-class k calls, we remind that channels are occupied either by new or handover calls. Furthermore, channels are occupied either until the end of service of a call or until a call is handed over to a transit cell. Since the channel holding time can be expressed as $t_{h1,k} = \min(t_{dk}, t_c)$ in the case of the source cell and $t_{h2,k} = \min(t_{dk}, T_c)$ in the case of a transit cell, then the mean value of $t_{hi,k}$, $E_k(t_{hi,k})$ for $i = 1, 2$ is given by

$$E_k(t_{hi,k}) = T_{dk}(1-P_{hi,k}). \tag{7}$$

We define now by P_k and P_k^h the probabilities that a channel is occupied by a new and a handover service-class k call, respectively. Then

$$P_k = \frac{\lambda_k(1-C_{b_k})}{\lambda_k(1-C_{b_k})+\lambda_{hk}(1-P_{f_k})} \tag{8}$$

and

$$P_k^h = \frac{\lambda_{hk}(1-P_{f_k})}{\lambda_k(1-C_{b_k})+\lambda_{hk}(1-P_{f_k})} \tag{9}$$

Based on (7)-(9), the channel holding time of service-class k calls (either new or handover) is approximated by an exponential distribution whose mean μ_k^{-1} is the weighted sum of (7) (for $i = 1, 2$) multiplied by the corresponding probabilities P_k (for $i = 1$) and P_k^h (for $i = 2$)

$$\mu_k^{-1} = P_k E_k(t_{h1,k}) + P_k^h E_k(t_{h2,k}) = \frac{\lambda_k(1-C_{b_k})E_k(t_{h1,k})}{\lambda_k(1-C_{b_k})+\lambda_{hk}(1-P_{f_k})} + \frac{\lambda_{hk}(1-P_{f_k})E_k(t_{h2,k})}{\lambda_k(1-C_{b_k})+\lambda_{hk}(1-P_{f_k})} \tag{10}$$

3. The analytical model

To analyze the LEO-MSS, each cell is modelled as a multirate loss system whereby all calls compete for the available channels under the CS policy. To facilitate the description of the analytical model, we distinguish new from handover calls and assume that each cell accommodates calls of $2K$ service-classes. A service-class k call is new if $1 \leq k \leq K$ and handover if $K+1 \leq k \leq 2K$. To this end, let the system be in steady state and denote by n_k the number of in-service calls (new or handover) of service-class k in a cell. Then, the steady state vector is defined as $\boldsymbol{n} = (n_1, ..., n_k, ..., n_{2K})$ and its corresponding probability distribution as $P_{\boldsymbol{n}}$.

We will show that $P_{\boldsymbol{n}}$ has a PFS. The latter is based on local flow balance through certain levels which separate the adjacent states of the form: a) $\boldsymbol{n}_k^{-1} = (n_1, \ldots, n_{k-1}, n_k - 1, n_{k+1}, \ldots, n_{2K})$ and $\boldsymbol{n}_k = (n_1, \ldots, n_k, \ldots, n_{2K})$ and b) $\boldsymbol{n}_k = (n_1, \ldots, n_k, \ldots, n_{2K})$ and $\boldsymbol{n}_k^{+1} = (n_1, \ldots, n_{k-1}, n_k + 1, n_{k+1}, \ldots, n_{2K})$. Let $L^{(k)}_{\boldsymbol{n}_k^{-1}}$ be the level that separates state $\boldsymbol{n}_k^{-1}$ from state $\boldsymbol{n}$ and $L^{(k)}_{\boldsymbol{n}}$ the level that separates state $\boldsymbol{n}$ from state $\boldsymbol{n}_k^{+1}$. Then, the "upward" (due to a new service-class k batch

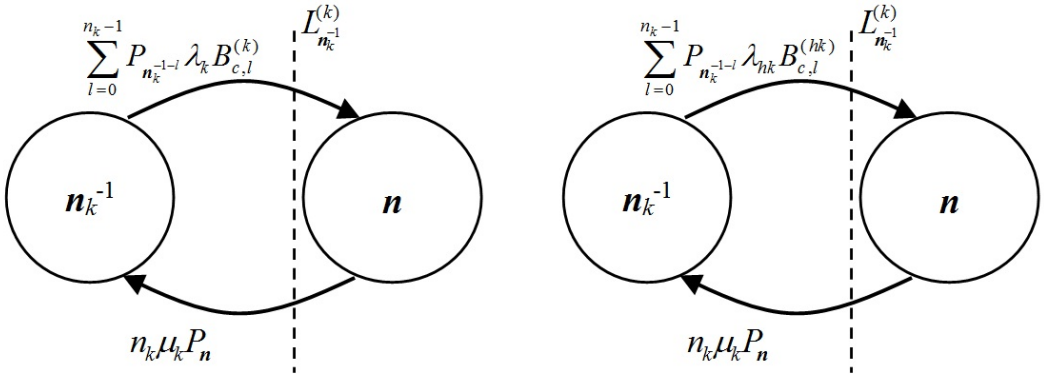

a *b*

Fig. 2: Local flow balance in the proposed model
a For new calls
b For handover calls

arrival or a handover service-class k call arrival), and the "downward" (due to a service-class k call departure) probability flows across $L_{\boldsymbol{n}_k^{-1}}^{(k)}$ are determined by

$$f^{(\text{up})}(L_{\boldsymbol{n}_k^{-1}}^{(k)}) = \begin{cases} \sum_{l=0}^{n_k-1} P_{\boldsymbol{n}_k^{-1-l}} \lambda_k B_{c,l}^{(k)}, k = 1, \ldots, K \\ \sum_{l=0}^{n_k-1} P_{\boldsymbol{n}_k^{-1-l}} \lambda_{hk} B_{c,l}^{(hk)}, k = K+1, \ldots, 2K \end{cases} \tag{11}$$

$$f^{(\text{down})}(L_{\boldsymbol{n}_k^{-1}}^{(k)}) = n_k \mu_k P_{\boldsymbol{n}}, k = 1, \ldots, 2K \tag{12}$$

where: $\boldsymbol{n}_k^{-1-l} = (n_1, \ldots, n_{k-1}, n_k - 1 - l, n_{k+1}, \ldots, n_{2K})$, with $n_k \geq 1 + l$ and $B_{c,l}^{(k)} = \sum_{m=l+1}^{\infty} B_m^{(k)}$, $B_{c,l}^{(hk)} = \sum_{m=l+1}^{\infty} B_m^{(hk)}$ are the complementary batch size distributions.

Based on (11) and (12), we have the following local flow balance equations between states $\boldsymbol{n}$ and $\boldsymbol{n}_k^{+1}$ for new $(k = 1, \ldots, K)$ and handover $(k = K+1, \ldots, 2K)$ calls, respectively (see also Fig. 2)

$$\sum_{l=0}^{n_k-1} P_{\boldsymbol{n}_k^{-1-l}} \lambda_k B_{c,l}^{(k)} = n_k \mu_k P_{\boldsymbol{n}}, k = 1, \ldots, K \tag{13}$$

$$\sum_{l=0}^{n_k-1} P_{\boldsymbol{n}_k^{-1-l}} \lambda_{hk} B_{c,l}^{(hk)} = n_k \mu_k P_{\boldsymbol{n}}, k = K+1, \ldots, 2K \tag{14}$$

The PFS that satisfies (13) and (14) is given by

$$P_{\boldsymbol{n}} = G^{-1} \left(\prod_{k=1}^{2K} P_{n_k}^{(k)} \right) \tag{15}$$

where G is the normalization constant, $G \equiv G(\boldsymbol{\Omega}) = \sum_{\boldsymbol{n}\in\boldsymbol{\Omega}} \left(\prod_{k=1}^{2K} P_{n_k}^{(k)} \right)$, $\boldsymbol{\Omega}$ is the state space of the system, $\boldsymbol{\Omega} = \{\boldsymbol{n} : 0 \leq \boldsymbol{nb} \leq C, k = 1, \ldots, 2K\}$, $\boldsymbol{nb} = \sum_{k=1}^{2K} n_k b_k$, $\boldsymbol{b} = (b_1, \ldots, b_{2K})^T$ and

$$P_{n_k}^{(k)} = \begin{cases} \sum_{l=1}^{n_k} \alpha_k \dfrac{P_{n_k-l}^{(k)} B_{c,l-1}^{(k)}}{n_k}, \text{ for } n_k \geq 1 \text{ and } k = 1, \ldots, K \\ \sum_{l=1}^{n_k} \alpha_{hk} \dfrac{P_{n_k-l}^{(k)} B_{c,l-1}^{(hk)}}{n_k}, \text{ for } n_k \geq 1 \text{ and } k = K+1, \ldots, 2K \\ 1, \text{ for } n_k = 0 \text{ and } k = 1, \ldots, 2K \end{cases} \tag{16}$$

where: $\alpha_k = \lambda_k/\mu_k$ and $\alpha_{hk} = \lambda_{hk}/\mu_k$ is the offered traffic-load (in erl).

An important batch size distribution is the geometric distribution, which is memoryless and a discrete equivalent of the exponential distribution. If new calls of service-class k arrive in batches of size s_k where s_k is geometrically distributed with parameter β_k, i.e., $\Pr(s_k = r) = (1-\beta_k)\beta_k^{r-1}$ with $r \geq 1$, then we have in (16), $B_{c,l-1}^{(k)} = \beta_k^{l-1}$. Similarly, we have $B_{c,l-1}^{(hk)} = \beta_{hk}^{l-1}$ for handover calls of service-class k.

To rely on (15), (16) for the determination of the various performance measures requires enumeration and processing of the state space. This task can be quite complex especially for a system of many service-classes and large capacity cells. On the other hand, (15) can be the springboard for the recursive calculation of the channel occupancy distribution, $q(j)$, where $j = \boldsymbol{nb} = \sum_{k=1}^{2K} n_k b_k$ is the number of occupied channels in a cell.

To this end, we multiply both sides of (13) by b_k and sum over $k = 1, \ldots, K$ to have

$$\sum_{k=1}^{K} \alpha_k b_k \sum_{l=0}^{n_k-1} P_{\boldsymbol{n}_k^{-1-l}} B_{c,l}^{(k)} = P_{\boldsymbol{n}} \sum_{k=1}^{K} n_k b_k \tag{17}$$

Similarly, by multiplying both sides of (14) by b_k and summing over $k = K+1, \ldots, 2K$ we obtain

$$\sum_{k=K+1}^{2K} \alpha_{hk} b_k \sum_{l=0}^{n_k-1} P_{\boldsymbol{n}_k^{-1-l}} B_{c,l}^{(hk)} = P_{\boldsymbol{n}} \sum_{k=K+1}^{2K} n_k b_k \tag{18}$$

Adding (17), (18) we have

$$\sum_{k=1}^{K} \alpha_k b_k \sum_{l=0}^{n_k-1} P_{\boldsymbol{n}_k^{-1-l}} B_{c,l}^{(k)} + \sum_{k=K+1}^{2K} \alpha_{hk} b_k \sum_{l=0}^{n_k-1} P_{\boldsymbol{n}_k^{-1-l}} B_{c,l}^{(hk)} = P_{\boldsymbol{n}} \left(\sum_{k=1}^{K} n_k b_k + \sum_{k=K+1}^{2K} n_k b_k \right) = j P_{\boldsymbol{n}} \tag{19}$$

In order to introduce $q(j)$ in (19), we sum both sides of (19) over $\boldsymbol{\Omega}_j = \{\boldsymbol{n} \in \boldsymbol{\Omega} : \boldsymbol{nb} = j\}$ where $\boldsymbol{\Omega}_j$ is the state space where exactly j channels are occupied by all in-service calls

$$\sum_{\boldsymbol{n}\in\boldsymbol{\Omega}_j} \sum_{k=1}^{K} \alpha_k b_k \sum_{l=0}^{n_k-1} P_{\boldsymbol{n}_k^{-1-l}} B_{c,l}^{(k)} + \sum_{\boldsymbol{n}\in\boldsymbol{\Omega}_j} \sum_{k=K+1}^{2K} \alpha_{hk} b_k \sum_{l=0}^{n_k-1} P_{\boldsymbol{n}_k^{-1-l}} B_{c,l}^{(hk)} = j \sum_{\boldsymbol{n}\in\boldsymbol{\Omega}_j} P_{\boldsymbol{n}} \tag{20}$$

By definition, we have

$$q(j) = \sum_{\boldsymbol{n} \in \boldsymbol{\Omega}_j} P_{\boldsymbol{n}} \tag{21}$$

Based on (21) and by interchanging the order of summations in (20), we have

$$\sum_{k=1}^{K} \alpha_k b_k \sum_{\boldsymbol{n} \in \boldsymbol{\Omega}_j} \sum_{l=0}^{n_k-1} P_{\boldsymbol{n}_k^{-1-l}} B_{c,l}^{(k)} + \sum_{k=K+1}^{2K} \alpha_{hk} b_k \sum_{\boldsymbol{n} \in \boldsymbol{\Omega}_j} \sum_{l=0}^{n_k-1} P_{\boldsymbol{n}_k^{-1-l}} B_{c,l}^{(hk)} = jq(j) \tag{22}$$

or

$$\sum_{k=1}^{K} \alpha_k b_k \sum_{l=1}^{\lfloor j/b_k \rfloor} q(j - l \times b_k) B_{c,l-1}^{(k)} + \sum_{k=K+1}^{2K} \alpha_{hk} b_k \sum_{l=1}^{\lfloor j/b_k \rfloor} q(j - l \times b_k) B_{c,l-1}^{(hk)} = jq(j) \tag{23}$$

since $\sum_{\boldsymbol{n} \in \boldsymbol{\Omega}_j} \sum_{l=0}^{n_k-1} P_{\boldsymbol{n}_k^{-1-l}} B_{c,l}^{(k)} = \sum_{l=1}^{\lfloor j/b_k \rfloor} q(j - l \times b_k) B_{c,l-1}^{(k)}$ and $\sum_{\boldsymbol{n} \in \boldsymbol{\Omega}_j} \sum_{l=0}^{n_k-1} P_{\boldsymbol{n}_k^{-1-l}} B_{c,l}^{(hk)} = \sum_{l=1}^{\lfloor j/b_k \rfloor} q(j - l \times b_k) B_{c,l-1}^{(hk)}$ while $\lfloor j/b_k \rfloor$ denotes the largest integer not exceeding j/b_k.

Having determined $q(j)$'s recursively via (23), we can calculate various performance measures including CBP and handover failure probabilities. More precisely, a new service-class k call is blocked and lost if the required b_k channels are not available in the cell upon its arrival. Based on (23), we determine CBP of new service-class k calls, C_{b_k}, via the formula

$$C_{b_k} = \frac{1}{G} \sum_{j=C-b_k+1}^{C} q(j) \tag{24}$$

where $G = \sum_{j=0}^{C} q(j)$ is the normalization constant.

Note that if all calls (new and handover) follow a Poisson process then we have the model of [13, 14]. In that case, (23) takes the form

$$\sum_{k=1}^{K} \alpha_k b_k q(j - b_k) + \sum_{k=K+1}^{2K} \alpha_{hk} b_k q(j - b_k) = jq(j) \tag{25}$$

while CBP of service-class k are given by (24).

In the proposed model, since the CS policy does not provide any priority to handover calls, we may assume that

$$P_{f_k} = C_{b_k} \tag{26}$$

To account for the successive handovers of a call during its lifetime in the system, (26) is modified to

$$P_{f_k} = \delta_k C_{b_k} \tag{27}$$

where δ_k is a correction factor introduced to model the dependency between successful handovers of a service-class k call prior to a handover failure. More precisely, a handover failure may occur during the $E_k(n_{hk})$th handover if an accepted call has already performed $E_k(n_{hk})-1$ successful handovers, i.e.

$$\delta_k = (1 - C_{b_k}) P_{h1,k} (1 - P_{f_k})^{E_k(n_{hk})-2} P_{h2,k}^{E_k(n_{hk})-2} \tag{28}$$

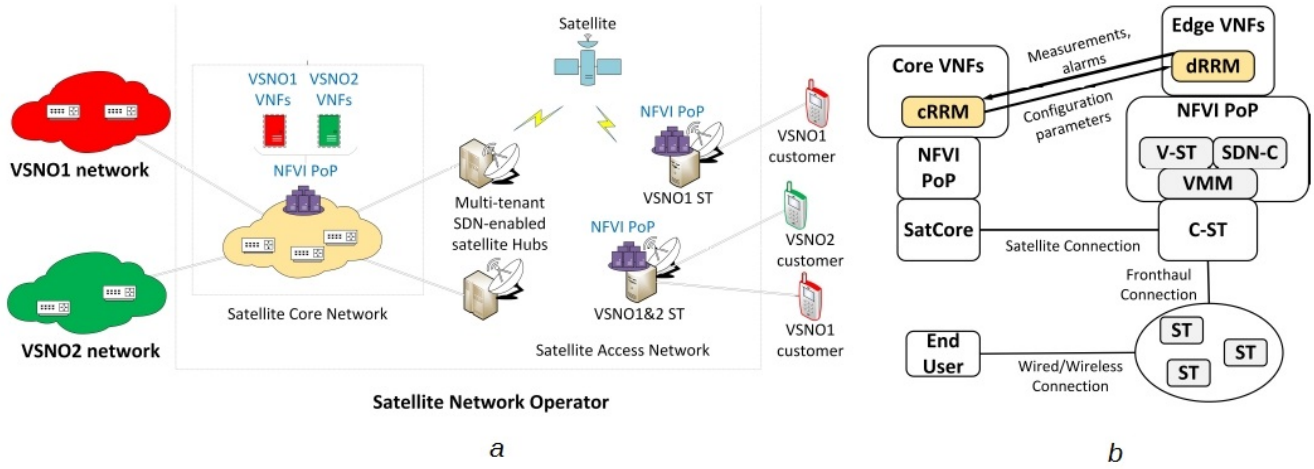

Fig. 3: A SDN/NFV enabled satellite network
a The architecture
b The radio resource management

where $E_k(n_{hk})$ is given by (for the proof see Appendix 2)

$$E_k(n_{hk}) = \frac{(1 - C_{b_k})P_{h1,k}}{1 - (1 - P_{f_k})P_{h2,k}} \tag{29}$$

To determine $q(j)$'s, C_{b_k} and P_{f_k} via (23), (24) and (27), the values of α_k, α_{hk}, are necessary. Since λ_{hk} and μ_k^{-1} depend on C_{b_k} and P_{f_k} an iterative procedure is necessary. The latter starts with $C_{b_k} = 0$ and stops when two consecutive values of C_{b_k} differ by less than 10^{-6}.

Having determined $q(j)$'s, C_{b_k} and P_{f_k}, the following performance measures can be calculated:

a) The call dropping probability of service-class k calls, P_{d_k}, which refers to new calls that are not blocked but are forced to terminate due to handover failure

$$P_{d_k} = \frac{P_{f_k}P_{h1,k}}{1 - P_{h2,k}(1 - P_{f_k})} \tag{30}$$

b) The unsuccessful call probability of service-class k calls, P_{us_k}, which refers to calls that are either blocked in the source cell or dropped due to a handover failure

$$P_{us_k} = C_{b_k} + P_{d_k}(1 - C_{b_k}) \tag{31}$$

4. Applicability of the proposed model in future LEO SDN/NFV satellite networks

4.1. Enabling SDN and NFV in future satellite networks

Our considered SDN/NFV satellite network architecture is presented in Fig. 3a. This is in line with the architecture proposed within the context of the EC H2020 VITAL project [23, 24]. In Fig. 3a, a satellite network operator (SNO) owns an SDN/NFV infrastructure that enables multi-tenancy. This means that the SNO may have multiple virtual SNOs (VSNOs) as its customers. On the other hand, the benefit for the VSNOs is that they can offer satellite services to their customers without owing any physical infrastructure.

In particular, our considered architecture consists of the following four parts:

- Control and management systems (to simplify the presentation, not shown in Fig. 3a). These include the network control center (NCC) and the network management center (NMC). The NCC typically provides real-time control of the satellite network, while the NMC is responsible for the management of the system elements in the network.
- Satellite core network. This connects the SNO's access network to the VSNOs' networks. The satellite core network includes NFV infrastructure (NFVI) points of presence (PoPs). On top of the NFVI, different tenants (i.e., VSNO1 and VSNO2 in this example) are able to install and operate their own virtual network functions (VNFs). Example of such VNFs are load balancers, firewalls, deep packet inspection (DPI) systems, etc. Typically, a satellite core network relies on the optical backbone network, where switching and equipment uses the IP/Multi-Protocol Label Switching (MPLS) protocol or Carrier Ethernet.
- Satellite access network. This consists of a cluster of SDN-enabled Hubs, connected to the satellite core network, and a distributed set of satellite terminals (STs), connected to the user equipment. Hubs and STs are interconnected via one or more channels (transponders) of a communication satellite. Both Hubs and STs are part of the NFVI. As shown in Fig. 3a, some STs can be multi-tenant, whereas others can be dedicated to a single VSNO.
- A constellation of LEO satellites. Its purpose is to connect Hubs to STs.

4.2. Applicability of the proposed model

In this subsection, we demonstrate the applicability of our proposed model in SDN/NVF enabled satellite networks. As a specific example, consider the virtualization of the radio resource management (RRM) function. This can be greatly facilitated by enhancing the network with self-organising network (SON) functionalities, which are fundamental to achieve an optimized network planning and operation [25]. A more autonomous and automated cellular network functionality, as enabled by SON, will result in simpler and faster decision-making and operation. Focusing on SON's self-optimization objective, the aim is to improve the network performance or keep it at an acceptable level. The optimisation could be performed in terms of QoS, coverage, and/or capacity improvements and is achieved by intelligently tuning various network settings (e.g., call admission control (CAC) thresholds) or at the SatCore level as well as at the ST level. One way to realize that is shown in Fig. 3b and is described below.

At the satellite core network (SatCore) level, the NFVI PoPs enable the execution of VNFs by the VSNOs. One such VNF could be a centralized RRM (cRRM) SON function that sets the appropriate configuration parameters to achieve, e.g., appropriate levels of QoS or CBP for VSNO's customers. On the other hand, at the satellite access network level, there is a distributed set of STs, which form a centralized pool of ST resources (C-ST) that is owned and controlled by the SNO. To benefit from NFV, the C-ST functionality and services have been abstracted from the underlying infrastructure and virtualized (V-ST). To realize the virtualization, the virtual machine monitor (VMM) is used to manage the execution of V-STs. The NFVI PoP also includes a SDN controller that is responsible for routing decisions and for configuring the packet forwarding elements. On top of the NFVI, a VSNO can execute a number of edge VNFs, such as the distributed RRM (dRRM) SON function.

As shown in Fig. 3b, the dRRM is logically connected to the cRRM. The cRRM sends to the dRRM various guidelines, configuration settings, and parameters. The cRRM determines the configuration parameters (e.g., CBP limits) based on a number of objectives (e.g., acceptable handover

failure probabilities, coverage requirements, capacity requirements, etc). The dRRM receives the configuration parameters (e.g., CBP limits) and acts accordingly (e.g., rejects connection requests that do not conform to the specified requirements). Also, the dRRM sends (at regular intervals or when a pre-defined condition is met) to the cRRM various performance measurements and alarms. For example, the dRRM may be configured to report the handover failure probabilities per service to the cRRM. If the reported measurements violate the objectives/performance constraints (e.g., QoS is below a predefined level or the handover failure probability for a particular service is too high), the cRRM will re-calculate and send updated configuration parameters to the dRRM.

5. Evaluation

In this section, we present an application example and provide analytical and simulation results of the CBP, the handover failure probability, the call dropping probability and the unsuccessful call probability for the proposed model. For comparison, we also present analytical results for the previous performance measures based on [13, 14], i.e., we consider Poisson arrivals and the CS, FCR policies.

For the simulation of the LEO-MSS we adopt the Iridium parameters. The simulated network consists of $N = 7$ contiguous cells (which is a typical value, see e.g., [26, 27]). Extensive simulations have shown that a higher value of N does not affect the simulation results. The subsatellite point speed is $V_{tr} = 26600$ km/h and the length of each cell is $L = 425$ km resulting in a maximum dwell time of a call in a cell equal to 57.5 s. MUs are uniformly distributed in the network of cells and new calls may arrive anywhere within the network. In addition, we do not consider distortion in the propagation links.

Simulation results are derived via the Simscript III simulation language [28] and are mean values of 7 runs. Confidence intervals of the results are found to be very small (less than two orders of magnitude) and they are not presented in Figs. 4-7.

In the application example, each cell has a capacity of $C = 30$ channels and accommodates batched Poisson arriving calls of $K = 2$ service-classes whose calls require $b_1 = 1$ and $b_2 = 2$ channels, respectively. The batch size of both service-classes follows the geometric distribution with two different sets of parameters: 1) $\beta_1 = \beta_2 = 0.2$ and 2) $\beta_1 = \beta_2 = 0.3$. The corresponding parameters for the handover calls of each service-class k is given by $\beta_k P_{h2,k}$ to account for the fact that the batched Poisson process of handover calls is actually less bursty than the corresponding arrival process of new calls. We further assume that $T_{d1} = 180$ s, $T_{d2} = 540$ s, while the offered traffic per cell is $\alpha_1 = 9$ erl and $\alpha_2 = 0.33$ erl. In the case of [13, 14] and the FCR policy, the FCR parameters for the new calls of each service-class are: $CR_1 = 1$ and $CR_2 = 0$ channels, respectively. This selection achieves CBP equalization among new calls of both service-classes, since $b_1 + CR_1 = b_2$.

In the x-axis of Figs. 4-7, the traffic loads α_1 and α_2 increase in steps of 0.5 and 0.05 erl, respectively. Thus, point 1 represents the offered traffic-load vector $(\alpha_1, \alpha_2) = (9.0, 0.33)$, while point 7 refers to the vector $(\alpha_1, \alpha_2) = (12.0, 0.36)$.

All figures show that:

- The batched Poisson process clearly results in much higher probability results compared to the corresponding results assuming the classical (and less bursty) Poisson process. This means that the existing models of [13, 14] fail to approximate the proposed model.
- The application of the FCR policy in the models of [13, 14] does not lead to results that are

close to the results obtained by the proposed model. This is anticipated, since the call arrival process in [13, 14] is smoother than the batched Poisson process. On the same hand, a channel allocation policy (e.g., the CS or the FCR policy) cannot capture the behavior of a call arrival process.

- An increase in the parameter β of the geometrical distribution results in an increase of the corresponding performance measures since the average number of calls in the arriving batches increases. Furthermore, as the values of β increase, the call arrival process becomes more bursty and the difference between the results obtained by the proposed model and the models of [13, 14] increases.
- Simulation results verify the accuracy of the proposed formulas.

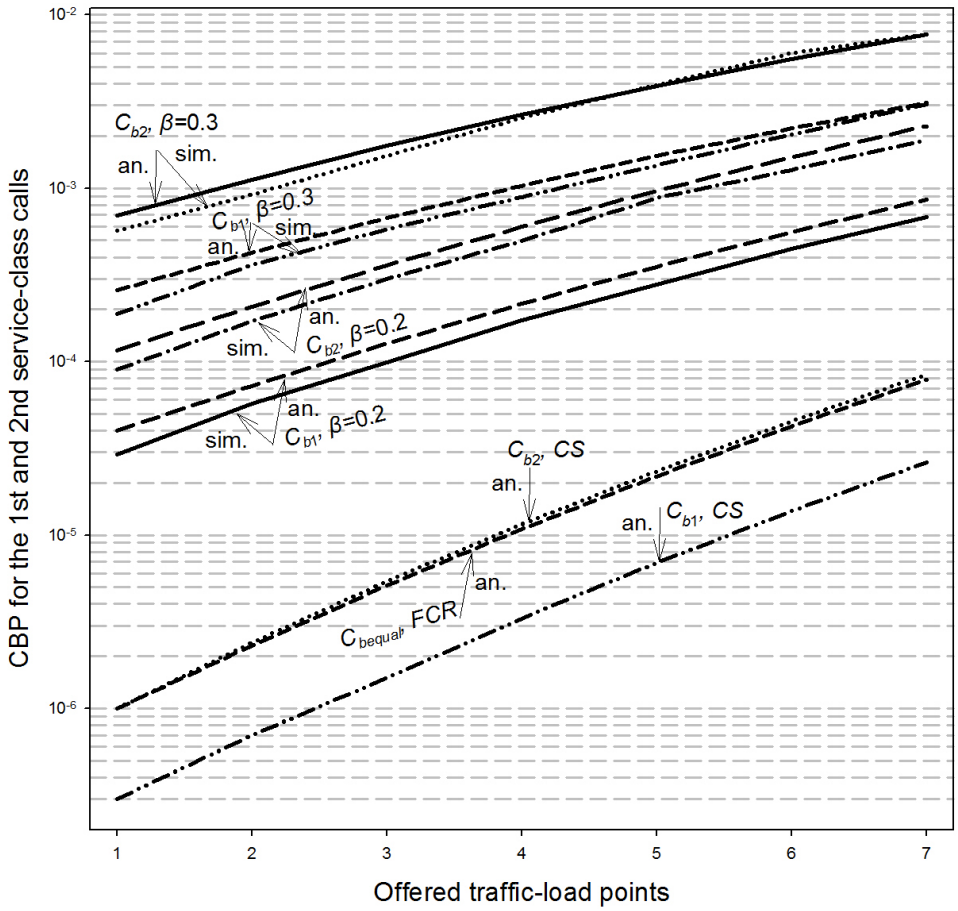

Fig. 4: CBP for both service-classes

6. Conclusion

In this paper, we concentrate on a LEO mobile satellite system with "satellite-fixed" cells and provide an analytical framework for the efficient calculation of various performance measures under

the assumption of batched Poisson arrivals for both new and handover calls. The proposed analytical model has a PFS which results in recursive and yet efficient formulas for the determination of the channel occupancy distribution and consequently for all performance measures. The analytical results of the proposed model show a high difference compared to the corresponding results when the classical Poisson process is considered. This fact reveals the necessity of the proposed model. The comparison of the analytical results obtained by the proposed model with the corresponding simulation results shows an absolutely satisfactory accuracy. Furthermore, we discuss the applicability of the proposed model in future LEO SDN/NFV enabled satellite networks. As a future work we intend to study: a) different call arrival processes for new and handover calls and b) the possibility of including operational times analysis for the LEO-MSS network in our teletraffic models.

7. Appendix 1: List of acronyms/abbreviations

CAC: Call Admission Control
CBP: Call Blocking Probabilities
CP: Complete Partitioning
cRRM: Centralized Radio Resource Management
CS: Complete Sharing
dRRM: Distributed Radio Resource Management
FCR: Fixed Channel Reservation
GB: Global Balance
LB: Local Balance
LEO: Low Earth Orbit
MSS: Mobile Satellite System
MU: Mobile User
NCC: Network Control Center
NFV: Network Function Virtualization
NFVI: Network Function Virtualization Infrastructure
NMC: Network Management Center
PFS: Product Form Solution
PoP: Point of Presence
QoS: Quality of Service
RRM: Radio Resource Management
SDN: Software-Defined Networking
SNO: Satellite Network Operator
ST: Satellite Terminal
TCA: Threshold Call Admission
VMM: Virtual Machine Monitor
VNF: Virtual Network Function
VSNO: Virtual Satellite Network Operator

8. Appendix 2

Let $E_k(n_{hk})$ be the average number of times that a new service-class k call is successfully handed over during its lifetime in the system and $P(n_{hk})$ the corresponding probabilities of having $n_{hk} =$

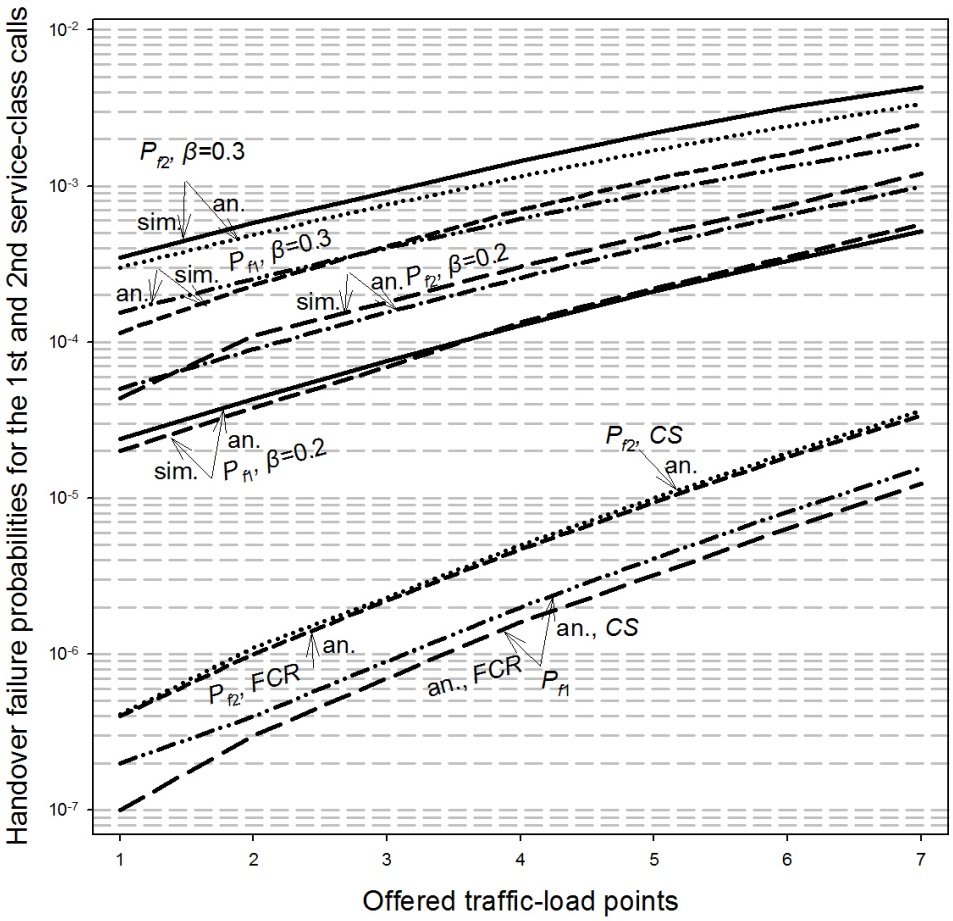

Fig. 5: Handover failure probabilities for both service-classes

$0, 1, 2, ...$ successful handovers. To determine $E_k(n_{hk})$ we work as follows

$$P(n_{hk} = 0) = (1 - P_{h1,k}) + P_{h1,k}P_{f_k} \tag{A1}$$

Equation (A1) refers to the probability of zero successful handovers. This is either because we do not have a handover from the source cell (this happens with probability $(1 - P_{h1,k})$) or because we have a handover with probability $P_{h1,k}$ but this is blocked with probability P_{f_k}.

On the same hand

$$P(n_{hk} = 1) = P_{h1,k}(1 - C_{b_k})(1 - P_{h2,k} + P_{h2,k}P_{f_k}) \tag{A2}$$

Equation (A2) refers to the probability of one successful handover. This is because the call is not blocked and we have one successful handover from the source cell to the first transit cell, expressed by $P_{h1,k}(1 - C_{b_k})$ "and either" we do not have a handover in the next transit cell (expressed by $1-P_{h2,k}$) "or" we have a handover in the next transit cell but it is blocked with probability $P_{h2,k}P_{f_k}$.

Similarly

$$P(n_{hk}=2)=P_{h1,k}(1-C_{b_k})P_{h2,k}(1-P_{f_k})(1 - P_{h2,k}+P_{h2,k}P_{f_k}) \tag{A3}$$

Equation (A3) refers to the probability of two successful handovers. This is because the call is not blocked and we have one successful handover from the source cell to the first transit cell with probability $P_{h1,k}(1 - C_{b_k})$ and a second successful handover from the first to the second transit cell with probability $P_{h2,k}(1 - P_{f_k})$. The last term shows that we do not have a handover in the next transit cell (expressed by $1 - P_{h2,k}$) "or" we have a handover in the next transit cell but it is blocked with probability $P_{h2,k}P_{f_k}$.

Similarly, for the case of $P(n_{hk} = 3)$ we have

$$P(n_{hk}=3)=P_{h1,k}(1-C_{b_k})\big(P_{h2,k}(1-P_{f_k})\big)^2(1-P_{h2,k}+P_{h2,k}P_{f_k}) \tag{A4}$$

or generally for the case of $P(n_{hk} = i)$

$$P(n_{hk}=i)=P_{h1,k}(1-C_{b_k})\big(P_{h2,k}(1-P_{f_k})\big)^{i-1}(1-P_{h2,k}+P_{h2,k}P_{f_k}) \tag{A5}$$

Thus based on (A5) and assuming that $Z = P_{h1,k}(1 - C_{b_k})(1 - P_{h2,k} + P_{h2,k}P_{f_k})$ we have $E_k(n_{hk}) = \sum_{i=1}^{\infty} iP(n_{hk} = i) = \sum_{i=1}^{\infty} iP_{h1,k}(1 - C_{b_k})\big(P_{h2,k}(1 - P_{f_k})\big)^{i-1}(1 - P_{h2,k} + P_{h2,k}P_{f_k}) =$ $Z\sum_{i=1}^{\infty} i\big(P_{h2,k}(1-P_{f_k})\big)^{i-1} \overset{x=P_{h2,k}(1-P_{f_k})}{=} Z\sum_{i=1}^{\infty} ix^{i-1} = Z\frac{1}{(1-x)^2} \Rightarrow E_k(n_{hk}) = \frac{(1-C_{b_k})P_{h1,k}}{1-(1-P_{f_k})P_{h2,k}}$ which is (29).

9. References

[1] Sun, Z: 'Satellite networking - principles and protocols' (2nd edition, John Wiley, 2014)

[2] Li, T., Zhou, H., Luo, H., Xu, Q., Ye, Y.: 'Using SDN and NFV to implement satellite communication networks', Proc. Int. Conf. Networking and Network Applications, Hokkaido, Japan, July 2016, pp. 131-134

[3] Yang, B., Wu, Y., Chu, X., Song, G.: 'Seamless handover in software-defined satellite networking', *IEEE Commun. Let.*, 2016, **20**, (9), pp. 1768-1771

[4] Maral, G., Restrepo, J., Del Re, E., Fantacci, R., Giambene, G.: 'Performance analysis for a guaranteed handover service in an LEO constellation with a 'satellite-fixed cell' system', *IEEE Trans. Veh. Tech.*, 1998, **47**, (4), pp. 1200-1214

[5] Zhou, J., Ye, X., Pan, Y., Xiao, F., Sun, L.: 'Dynamic channel reservation scheme based on priorities in LEO satellite systems', *Journal of Systems Engineering and Electronics*, 2015, **26**, (1), pp. 1-9

[6] Wang, Z., Mathiopoulos, P.: 'Analysis and performance evaluation of dynamic channel reservation techniques for LEO mobile satellite systems', Proc. IEEE VTC Spring, Rhodes, Greece, May 2001, pp. 2985-2989

[7] Bouchatem, L., Gaiti, D., Pujolle, G.: 'TCRA: A Time-based channel reservation scheme for handover requests in LEO satellite systems', *Int. J. Satell. Commun. Netw.*, 2003, **21**, (3), pp. 227-240

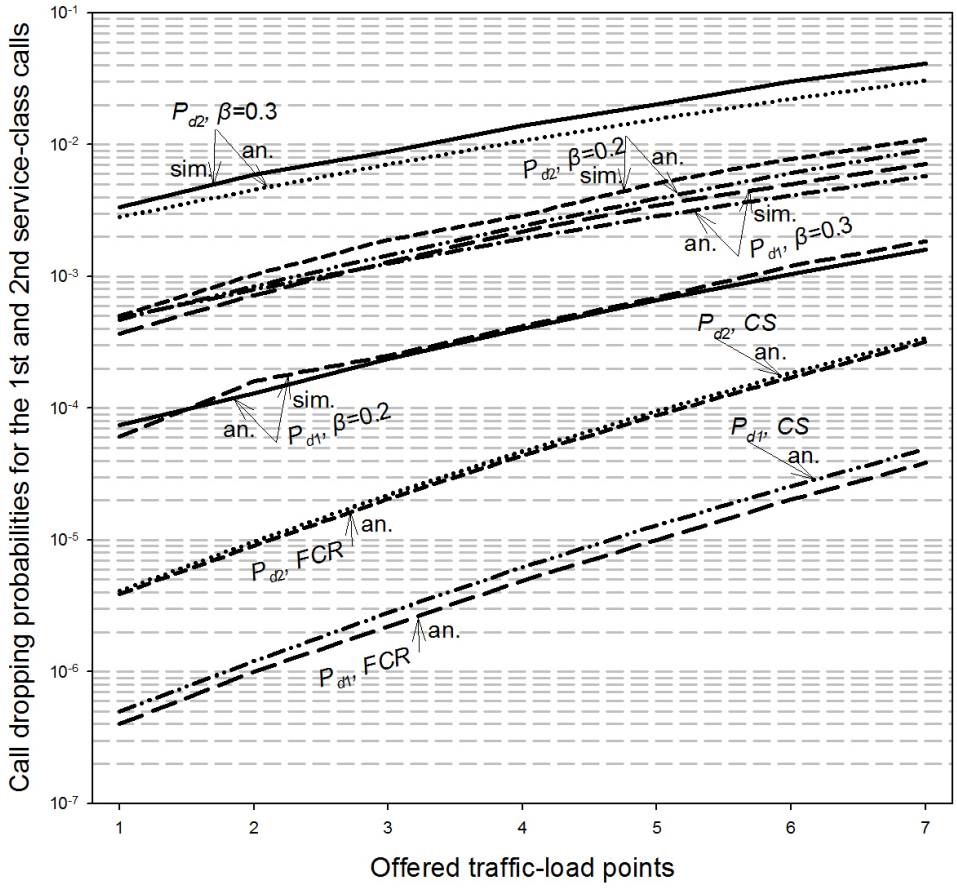

Fig. 6: Call dropping probabilities for both service-classes

[8] Wang, X. Wang, X.: 'The research of channel reservation strategy in LEO satellite network', Proc. 11th IEEE Int. Conf. Dependable, Autonomic and Secure Computing, Chengdu, China, Dec. 2013, pp. 590-594

[9] Papapetrou, E., Pavlidou, F-N.: 'Analytic study of Doppler-based handover management in LEO satellite systems', *IEEE Trans. Aerospace and Electronics Systems*, 2005, **51**, (3), pp. 830-839

[10] Karapantazis, S., Pavlidou, F-N.: 'Dynamic time-based handover management in LEO satellite systems', *Electronics Letters*, 2007, **43**, (5), pp. 57-58

[11] Chen, L., Guo, Q., Wang, H.: 'A handover management scheme based on adaptive probabilistic resource reservation for multimedia LEO satellite networks', Proc. Int. Conf. Information Engineering, BeiDai, China, August 2010, pp. 255-259

[12] Liao, M., Liu, Y., Hu, H., Yuan, D.: 'Analysis of maximum traffic intensity under pre-set quality of service requirements in low earth orbit mobile satellite system for fix channel reservation with queueing handover scheme', *IET Commun.*, 2015, **9**, (13), pp. 15751582

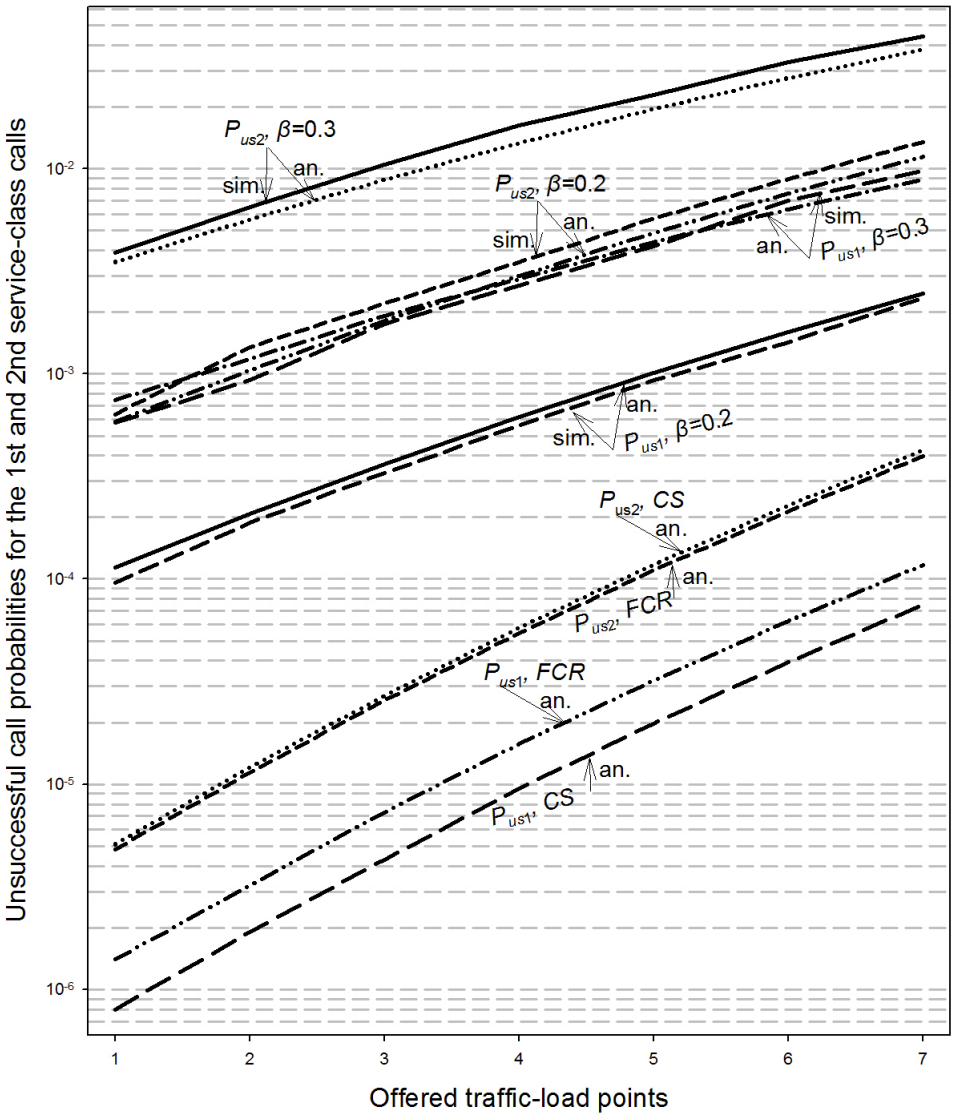

Fig. 7: Unsuccessful call probabilities for both service-classes

[13] Wang, Z., Mathiopoulos, P., Schober, R.: 'Performance analysis and improvement methods for channel resource management strategies of LEO-MSS with multiparty traffic', *IEEE Trans. Veh. Tech.*, 2008, **57**, (6), pp. 3832-3842

[14] Wang, Z., Mathiopoulos, P. Schober, R.: 'Channeling Partitioning Policies for Multi-Class Traffic in LEO-MSS', *IEEE Trans. Aerospace and Electronic Systems*, 2009, **45**, (4), pp. 1320-1334

[15] Wang, Z., Makrakis, D., Mouftah, H.: 'Performance Analysis of Threshold Call Admission Policy for Multi-class Traffic in Low Earth Orbit Mobile Satellite Systems', Proc. 2nd Int. Conf. Advances in Satellite and Space Communications, Athens, Greece, June 2010, pp. 52-57

[16] Paxson, V., Floyd, S.: 'Wide area traffic: the failure of Poisson modeling', *IEEE/ACM Trans. Netw.*, 1995, **3**, (3), pp. 226-244

[17] Celandroni, N., Ferro, E., Gotta, A.: 'RA and DA satellite access schemes: a survey and some research results and challenges', *Int. J. Commun. Syst.*, 2014, **27**, (11), pp. 2670-2690

[18] Arcidiacono, A., et. al.: 'From S-band mobile interactive multimedia to fixed satellite interactive multimedia: making satellite interactivity affordable at Ku-band and Ka-band', *Int. J. Satell. Commun. Netw.*, 2016, **34**, (4), pp. 575-601

[19] Wolff, R.: 'Stochastic modelling and the theory of queues' (Prentice Hall, 1989)

[20] Benslama, M., Kiamouche, W., Batatia,H.: 'Connections Management Strategies in Satellite Cellular Networks', (John Wiley, 2015)

[21] Del Re, E., Fantacci, R., Giambene, G.: 'Performance analysis of dynamic channel allocation technique for satellite mobile cellular networks', *Int. J. Satell. Commun.*, 1994, **12**, (1), pp. 2532

[22] Stasiak, M., Glabowski, M., Wisniewski, A., Zwierzykowski, P.: 'Modeling and Dimensioning of Mobile Networks', (John Wiley, 2011)

[23] Ferrs, R., Koumaras, H., Sallent, O., Agapiou, G., Rasheed, T., Kourtis, M-A., Boustie, C., Glard, P., Ahmed, T.: 'SDN/NFV-enabled satellite communications networks: opportunities, scenarios and challenges', *Physical Commun.*, 2016, **18**, (2), pp. 95-112

[24] EC H2020 VITAL (VIrtualized hybrid satellite-TerrestriAl systems for resilient and fLexible future networks) project, www.ict-vital.eu/ (accessed: Mar. 2017).

[25] 3GPP 32.500 v12.1.0, 'Self-Organizing Networks (SON); Concepts and requirements (Release 12),' Sept. 2014

[26] Del Re, E., Fantacci, R., Giambene, G.: 'An efficient technique for dynamically allocating channels in satellite cellular networks', Proc. IEEE Globecom, Singapore, Nov. 1995, pp. 1624-1628

[27] Wang, Z., Mathiopoulos, P.: 'On the performance analysis of dynamic channel allocation with FIFO handover queueing in LEO-MSS', *IEEE Trans. Commun.*, 2005, **53**, (9), pp. 1443-1446

[28] Simscript III, http://www.simscript.com (accessed: June 2017).